

SPONTANEOUS GROWTH OF AN IN-PLANE SHEAR CRACK†

A. K. CHATTERJEE AND L. KNOPOFF

Institute of Geophysics and Planetary Physics, University of California, Los Angeles, CA 90024, USA

(Received 27 April 1983; in revised form 30 January 1984)

Abstract—We consider the nonsteady growth of a two-dimensional in-plane shear crack under the influence of a critical stress intensity factor criterion at the crack tips and dynamical frictional stresses on the fracture surface. For a spontaneous rupture initiating at a point and extending bilaterally, the dynamic stress distribution must be known in advance to determine the stress intensities at the crack tips. When these stresses are scaled with respect to the singular stresses at the respective crack tips, an approximation that was found to be suitable for problems of the growth of anti-plane shear cracks that tear with high velocities, is also found to be suitable in the present case. The region of validity of this approximation is tested for the in-plane mode of crack growth by comparison with cases of crack histories that are solvable exactly. For the latter purpose, we use the exact solution to the self-similar problem of uniform bilateral growth of in-plane cracks, which is found by functionally invariant methods. For low rupture speeds, iterative methods based on this approximation can be developed to improve the solution. For the self-similar cases, rupture velocities cannot be greater than the Rayleigh wave velocity in the medium; we have only considered those cases of non-uniform crack propagation for which this limit also applies.

1. INTRODUCTION

The dynamics of a two-dimensional fracture that initiates at a point and extends along a plane fault in an otherwise homogeneous elastic medium, has been studied in some detail as a model for shallow focus earthquakes [1-4]. Previously Knopoff and Chatterjee [4] and Chatterjee and Knopoff [5] (henceforth referred to as I and II respectively) have considered the problem of the anti-plane mode of shear fracture where critical fracture strengths at the crack tips have been taken into account. In this paper, we discuss this problem for the case of the in-plane mode of fracture. The anti-plane problem can be formulated in terms of an integral equation for motions of the SH-type in seismological notation; in the present case, dual integral equations are encountered which couple P and SV motions.

To date, analytical solutions of problems of the extension of two-dimensional plane strain shear cracks under the influence of cohesive forces at the crack tips have been limited to the analysis of the growth of semi-infinite cracks ([2, 6, 7], for example) and the growth of finite cracks ([6] and others). Andrews [3] offers the conjecture that cracks with extension rates v_c bounded by $0 < v_c < v_R$ and $2^{1/2}\beta < v_c < \alpha$ are stable, where α , β and v_R are the P -, S - and Rayleigh wave velocities in the medium respectively. On the other hand, through the use of a point force load near the tip of a semi-infinite crack, Burridge *et al.* [7] have found contradictory results, namely that the region $2^{1/2}\beta < v_c < \alpha$ is stable while the regions $0 < v_c < v_R$, $\beta < v_c < 2^{1/2}\beta$ are unstable and the region $v_R < v_c < \beta$ is forbidden; stability implies that the velocity of extension of the crack decreases with increase in the load and conversely instability implies that the crack speeds up with increase of load.

The release of a constrained semi-infinite crack at $t = 0$ represents a set of initial conditions that may be physically unrealistic. The development of a crack initiating at a point is probably more realistic physically especially from the point of view of modelling of earthquake sources than is the problem of a pre-existing semi-infinite crack. We wish to test whether the conclusions drawn from models of extension of semi-infinite cracks are applicable to growing point-source problems.

† Publication No. 2496. Institute of Geophysics and Planetary Physics, University of California, Los Angeles, California 90024.

In the case of cracks that initiate at a point, the elastic wave radiation from one end of a crack influences the stress configuration of the opposite edge. We find that the stress field radiated by one edge always causes the rate of extension of the opposite edge to be reduced. The rates of extension in the early phases of growth of these cracks are always less than the Rayleigh wave velocity in the medium. This does not mean that higher rates of extension are excluded in the latter phases of growth histories. On the contrary, since the stress fields can propagate with velocities up to the P -wave velocity, it is possible that triggering of crack segments at rates up to the P -wave velocity can take place in a suitably inhomogeneous distribution of strength and prestress.

To model the dynamical shear fracture of cracks with moving edges, we need an adequate fracture criterion. The solution of a differential equation with moving boundaries is sensitive to the choice of boundary conditions. In our case, the forces near the crack tips are modelled as cohesive forces. While the cohesive forces due to molecular bonding are of negligible importance on the scale of fractures appropriate for an earthquake, the effects of the geometry of fracture surfaces provide an equivalent set of cohesive stresses. Real earthquake faults as well as other real fracture surfaces are not ideal planes but instead consist of a series of geometrical irregularities [8–10]; the scale of self-similarity ranges over many orders of magnitude. In order that fractures on one segment of a complex fracture surface can trigger motions on a nearby segment, sufficient stresses must be available near the crack tip. We model the distribution of stresses needed to trigger motions on adjacent segments as a distribution of critical stresses on an equivalent plane fault. If the critical stress is too high to be overcome by the dynamically generated stress at the crack tip, the crack stops and leaves behind a large residual stress frozen into the region near the crack tip. These residual stresses can be involved in the production of aftershocks. Since the edges of our cracks will be modeled as points, i.e. there is no transition zone to support cohesive forces, the stresses in the neighborhood of an edge varies as $Kr^{-1/2}$ where r is the distance from the edge. We impose the fracture criterion that the stress intensity factor K generated at an advancing edge of the crack be greater than a property of material K_{mat} in order that the crack continues to extend. Additional details regarding this model can be found in II. (In the present calculation, the quantity K_{mat} is assumed to have a smooth distribution for the purpose of attaining an understanding of the underlying physics and mathematics.) Thus our fracture criterion requires that the stress generated by the advancing crack be greater than or equal to the strength of the material in front of it in order that it continues to advance. We adopt the above (singular) form of this statement to accommodate for the mathematical convenience afforded by allowing the edges of the crack to be points.

The problem of the propagation of a spontaneous crack initiating at a point is significantly different from that of the extension of semi-infinite cracks or cracks of finite initial length. In the latter cases, the crack tip stresses can be completely determined when the dynamical stress drop is known. But for a crack initiating at a point, the crack tip stress intensities depend on the unknown distribution of stresses ahead of the crack tip, which are themselves dependent on both crack edge locus histories. Thus, in these problems, the cracks enter regions which are not only prestressed statically but are also dynamically prestressed due to the radiation from the motions between both edges of the crack. Purely numerical attacks on these nonlinear dynamic crack problems have been given ([2] and others) but no exact analytical solutions are available for an arbitrary distribution of cohesions and dynamic stress drop. In the case of the anti-plane mode of fracture, we have given an exact iterative solution for the stress fields between the S -wave fronts and the crack tips which advance with sub- S -wave velocity. The stresses in this spatial interval, scaled by the stresses at the crack tips, can be represented by a function which is zero at the S -wave front, and unity at the crack front. To first order, this function can be assumed to be linear (I and II). It has been shown that, except for very slow rates of extension of the crack, this approximation yields solutions for rupture

histories that are very close to the exact solution, at least for cases of self-similar uniform propagation of cracks, for which exact analytical solutions are available.

In this paper we discuss the possibility of applying this approximation to the determination of the stresses outside the torn region for in-plane shear crack propagation under the influence of cohesion and dynamic friction. We believe that this method provides a better computational alternative, and may impart more physical insight to the problem than the purely numerical methods considered previously. For slow rates of extension of cracks, the solutions obtained from the approximate procedure can be used as initial estimates for an iteration which converges rapidly to the exact solution.

Below we show that the Rayleigh wave velocity is the maximum velocity of rupture of a self-similar crack and in the early stages of growth of a non-uniform crack. Thus the loading functions for these cracks form a transitional state between stability and instability. For material stress intensity factor K_{mat} that grows at a rate greater than the critical rate necessary for self-similarity, the cracks may be expected to slow down and for K_{mat} that grows at a rate less than these critical rates cracks may be expected to speed up and may even have velocities approaching α [11].

2. IN-PLANE MODE OF FRACTURE OF A BILATERAL CRACK

Consider an isotropic elastic medium with α , β and v_R representing the P -, S - and Rayleigh wave velocities respectively. Let a crack initiate spontaneously along the line $x = z = 0$ (Fig. 1) and propagate bilaterally along the $\pm x$ -axis. Suppose that after time t the crack occupies the region

$$\begin{aligned} z = 0, \quad -\infty < y < \infty \\ l_-(t) \leq x \leq l_+(t). \end{aligned} \quad (2.1)$$

For the plane strain problem, the displacement components (u , w) are functions of x , z and t ; the anti-plane component of motion $v = 0$. All of the stresses and displacements are continuous across the plane of the crack $z = 0$ except that u is discontinuous within the above interval. The equations of motion are

$$\begin{aligned} \ddot{u} &= \beta^2 [m^{-2} u_{,xx} + u_{,zz} + (m^{-2} - 1) w_{,xz}] \\ \ddot{w} &= \beta^2 [m^{-2} w_{,zz} + w_{,xx} + (m^{-2} - 1) u_{,xz}] \end{aligned} \quad (2.2)$$

where $m = \beta/\alpha$, the comma indicates spatial differentiation with respect to the variables indicated and the overhead dot indicates time derivative. The relevant components of

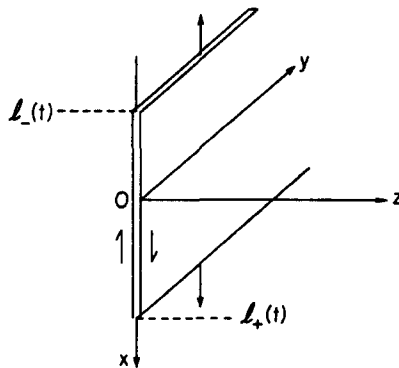


Fig. 1. Geometry of in-plane crack at $t > 0$. Initiation is at the y -axis. Crack is infinite in the y -direction and extends in the $\pm x$ -direction. The displacement on the crack faces is in the $\pm x$ -directions.

the stress tensor are

$$\begin{aligned} \sigma_{xx} &= \mu[m^{-2}u_{,x} + (m^{-2} - 2)w_{,z}] \\ \sigma_{zz} &= \mu[m^{-2}w_{,z} + (m^{-2} - 2)u_{,x}] \\ \sigma_{xz} &= \mu(u_{,z} + w_{,x}) \end{aligned} \tag{2.3}$$

where μ is the shear modulus.

We describe the deviations of all quantities from their values in the prestressed state $t < 0$. Accordingly, we prescribe the following boundary conditions:

- (i) $\sigma_{xz}(x, 0, t) = -f(x, t)$, $z = 0$, $l_-(t) < x < l_+(t)$
- (ii) w is continuous across $z = 0$
- (iii) u is continuous outside the crack

$$[u] = 0, \quad z = 0, \quad x < l_-(t), \quad x > l_+(t) \tag{2.4}$$

where $[u](x, t) = u(x, 0^+, t) - u(x, 0^-, t)$; $[u]$ is nonzero inside the above interval. The function $[u]$ is anti-symmetric in z and hence we only need consider the region $z \geq 0$; we set $[u] = 2u(x, 0^+, t)$. All the stresses and displacements approach zero as $z \rightarrow \pm\infty$.

The solution to the problem follows Kostrov [6] who has performed a significant amount of expository mathematics. Kostrov has studied the extension of semi-infinite and initially finite cracks under in-plane stresses. The notation and mathematics developed therein are of use in our case as well. Two transformations $f^{(1)}(x, t; s)$ and $f^{(2)}(x, t; s)$ of a given function $f(x, t)$ can be defined by

$$\begin{aligned} f^{(1)} &= \frac{\partial}{\partial t} \int_0^{t/s} f(x - \eta, t - s\eta) d\eta = I^{(1)} \\ f^{(2)} &= \frac{\partial}{\partial t} \int_0^{t/s} f(x + \eta, t + s\eta) d\eta = I^{(2)}. \end{aligned} \tag{2.5}$$

The integrals $I^{(1),(2)}$ in (2.5) are evaluated in the x - t plane along lines through (x, t) , which make angles $\pm \tan^{-1} s$ with the positive x -axis (Fig. 2).

Let $\sigma_2(x, t)$ be the shear stress in the plane of the crack, $\sigma_{xz}(x, 0, t) = \sigma_2(x, t)$; $\sigma_2(x, t)$ is known in the interval $l_-(t) < x < l_+(t)$ through (2.4). Four functions $F_{\pm}(x, t)$

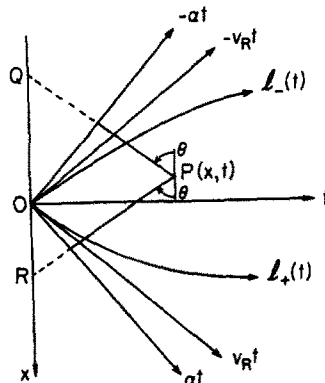


Fig. 2. The lines of integration for $I^{(1)}$ and $I^{(2)}$ are PQ and PR respectively. The dashed parts lie in the undisturbed regions and do not contribute to the integrals. The angle $\theta = \tan^{-1} s$.

and $G_{\pm}(x, t)$ are introduced which are defined in terms of the stress $\sigma_2(x, t)$ and displacement $[u](x, t)$ through

$$F_+(x, t) = \sigma_2(x, t) - (v_R^{-1} - \alpha^{-1})^{1/2}(v_R^{-1} - \beta^{-1})^{1/2}\sigma_2^{(1)}(x, t; v_R^{-1})/S(-v_R^{-1}) - \frac{1}{2\pi} \int_{\alpha^{-1}}^{\beta^{-1}} \frac{\{1/S(-s)\}(s - \alpha^{-1})^{1/2}(\beta^{-1} - s)^{1/2}\sigma_2^{(1)}(x, t; s)}{(v_R^{-1} - s)} ds \quad (2.6a)$$

$$G_+(x, t) = \frac{\mu}{4}(1 - m^2) \left[[u](x, t) \right. \quad (2.6b)$$

$$\left. + \frac{1}{\pi} \int_{\alpha^{-1}}^{\beta^{-1}} \frac{(v_R^{-1} - s)\{S(-s)\}}{(s - \alpha^{-1})^{1/2}(\beta^{-1} - s)^{1/2}} [u^{(2)}](x, t; s) ds \right] \quad (2.6c)$$

$$\sigma_2(x, t) = F_+(x, t) + \frac{1}{2\pi} \int_{\alpha^{-1}}^{\beta^{-1}} \frac{(v_R^{-1} - s)\{S(-s)\}}{(s - \alpha^{-1})^{1/2}(\beta^{-1} - s)^{1/2}} [F_+^{(1)}](x, t; s) ds$$

$$[u](x, t) = \frac{4}{\mu(1 - m^2)} \left[G_+(x, t) - (v_R^{-1} - \alpha^{-1})^{1/2}(v_R^{-1} - \beta^{-1})^{1/2}G_+^{(2)}(x, t; v_R^{-1})/S(-v_R^{-1}) - \frac{1}{2\pi} \int_{\alpha^{-1}}^{\beta^{-1}} \frac{\{1/S(-s)\}(s - \alpha^{-1})^{1/2}(\beta^{-1} - s)^{1/2}}{(v_R^{-1} - s)} G_+^{(2)}(x, t; s) ds \right] \quad (2.6d)$$

with four additional equations obtained by replacing the subscripts + by - and interchanging the superscripts (1) and (2). Kostrov [6] has shown that

$$\frac{\bar{F}_{\pm}(q, p)}{p(\alpha^{-2} - q^2 p^{-2})^{1/2}} + \bar{G}_{\pm}(q, p) = 0. \quad (2.7)$$

In (2.6) $\{f(x)\} = f(x + i0) + f(x - i0)$ for any function $f(x)$, and $S(\pm s)$ are the Wiener-Hopf decomposition factors of the Rayleigh denominator $R(s)$ and are given by [12]

$$R(s) = 2(\beta^{-2} - \alpha^{-2})(v_R^{-2} - s^2)S(s)S(-s) \quad (2.8)$$

where

$$S(s) = \exp \left[-\frac{1}{\pi} \int_{\alpha^{-1}}^{\beta^{-1}} \tan^{-1} \left\{ \frac{4k^2(k^2 - \alpha^{-2})^{1/2}(\beta^{-2} - k^2)^{1/2}}{(2k^2 - \alpha^{-2})^2} \right\} \frac{dk}{k + s} \right]. \quad (2.9)$$

For the anti-plane strain mode of fracture, the relationship between the transformed stress drop $\sigma_{yz}(q, 0, p) = \sigma_{yz}(q, p)$ and the displacement discontinuity $[\bar{v}](q, p)$ has been found to be [6]

$$\frac{\bar{\sigma}_{yz}(q, p)}{p(\beta^{-2} - q^2 p^{-2})^{1/2}} + \frac{\mu}{2} [\bar{v}](q, p) = 0$$

which is similar to (2.7).

Since $[u](x, t) = 0$ for $x > l_+(t)$, it follows from (2.6b) that (Fig. 3)

$$G_+(x, t) = 0, \quad x > l_+(t). \quad (2.10a)$$

Similarly

$$G_-(x, t) = 0, \quad x < l_-(t). \quad (2.10b)$$

From (2.7) and (2.10) we see that the problem of the in-plane shear crack has been

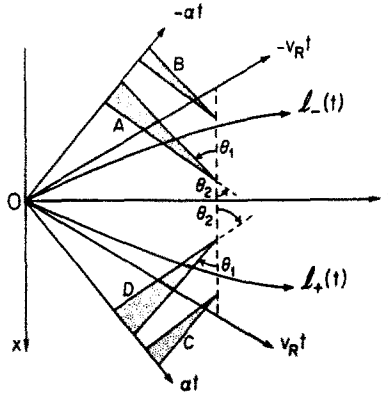


Fig. 3. Regions of integration for the determination of F_{\pm} and G_{\pm} . Triangles A, B identify the regions of integration for the integral in (2.6a) for $x \geq l_-(t)$ respectively while C and D identify the regions of integration for the integral in (2.6b) for $x \geq l_+(t)$. The angles $\theta_1 = \tan^{-1}(\alpha^{-1})$ and $\theta_2 = \tan^{-1}(\beta^{-1})$.

reduced to that of the anti-plane crack in which the characteristic velocity is changed from the S -wave velocity β to the P -wave velocity α . This enables us to write down the stress intensity factors for the in-plane problem and accordingly the fracture criterion in terms of $F_+(x, t)$ and $F_-(x, t)$. For the determination of these functions we use (2.5) and (2.6) where the unknown stresses $\sigma_2(x, t)$ outside the rupture zone are approximated by the approximation in I and II.

3. STRESS INTENSITY FACTORS AT THE CRACK TIPS

Let us assume that

$$F_+(x, t) = \frac{g^{(m)+}}{\pi[x - l_+(t)]^{1/2}} + 0(1) \tag{3.1a}$$

$$F_-(x, t) = \frac{g^{(m)+}}{\pi[x - l_+(t)]^{1/2}} + 0(1) \tag{3.1b}$$

$$\sigma_2(x, t) = \frac{g_+}{\pi[x - l_+(t)]^{1/2}} + 0(1) \tag{3.1c}$$

as $x \rightarrow l_+(t)^+$ and

$$F_+(x, t) = \frac{g^{(m)-}}{\pi[l_-(t) - x]^{1/2}} + 0(1) \tag{3.2a}$$

$$F_-(x, t) = \frac{g^{(m)-}}{\pi[l_-(t) - x]^{1/2}} + 0(1) \tag{3.2b}$$

$$\sigma_2(x, t) = \frac{g_-}{\pi[l_-(t) - x]^{1/2}} + 0(1) \tag{3.2c}$$

as $x \rightarrow l_-(t)^-$.

The superscripts (m) for the functions g , represent the modified stress intensity factors while the first subscript identifies the F function and the second subscript indicates the crack edge. Thus, for example, $g^{(m)+}$ is the modified stress intensity factor for F_+ at the positive edge of the crack. In these expressions we have assumed that the stresses F and σ have the well-known reciprocal square root singularity just beyond the appropriate edges of the crack, which is a property of cracks with sharp linear edges. Equations (3.1c) and (3.2c) indicate the self-regulating character of the growth

of the crack and describe the condition for the extension of the crack. The coefficients of cohesion g_{\pm} are measures of the ability of the material at the edges of the crack to absorb singular stresses and are properties of the material that are presumed to be specified in advance. If the dynamically generated stresses are less than the first term on the right hand side of (3.1c) or (3.2c), then the extension of the crack ceases. Thus (3.1c) and (3.2c) describe the critical stress intensity fracture criterion for the extension of the crack tips. We show below that self-similar cracks extend with velocity less than the Rayleigh wave velocity. We consider here only those cases of non-uniform crack extension for which $|\dot{l}_{\pm}| \leq v_R$.

Equations (2.6) give

$$\begin{aligned} g_{+,+}^{(m)} &= g_+ f_1(\dot{l}_+) \\ g_{+,-}^{(m)} &= g_- f_1(\dot{l}_-) \\ g_{-,+}^{(m)} &= g_+ f_1(-\dot{l}_+) \\ g_{-,-}^{(m)} &= g_- f_1(-\dot{l}_-) \end{aligned} \tag{3.3}$$

where

$$f_1(x) = \frac{(1 - x\alpha^{-1})^{1/2}(1 - x\beta^{-1})^{1/2}}{S(-x^{-1})(1 - xv_R^{-1})} \tag{3.4}$$

Inverting (2.7), we have (Fig. 4)

$$G_{\pm}(\xi_0, \eta_0) = -\frac{1}{2\pi} \int_0^{\xi_0} \int_0^{\eta_0} \frac{F_{\pm}(\xi, \eta) d\xi d\eta}{[(\xi_0 - \xi)(\eta_0 - \eta)]^{1/2}} \tag{3.5}$$

where ξ, η are the characteristic coordinates defined in terms of the P -wave velocity as

$$\begin{aligned} \xi &= \alpha t + x \\ \eta &= \alpha t - x. \end{aligned} \tag{3.6}$$

We let $\xi = \xi_-(\eta)$ or $\eta = \eta_-(\xi)$ be the coordinates of the negative crack edge $x = l_-(t)$ and $\xi = \xi_+(\eta)$ or $\eta = \eta_+(\xi)$ be those for the positive crack edge $x = l_+(t)$. Then from (2.10) and (3.5), it follows that

$$\int_0^{\xi_0} \frac{F_+(\xi, \eta_0) d\xi}{(\xi_0 - \xi)^{1/2}} = 0, \quad \xi_0 > \xi_+(\eta_0) \tag{3.7a}$$

$$\int_0^{\eta_0} \frac{F_-(\xi_0, \eta) d\eta}{(\eta_0 - \eta)^{1/2}} = 0, \quad \eta_0 > \eta_-(\xi_0). \tag{3.7b}$$

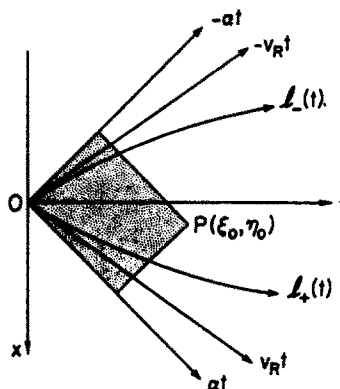


Fig. 4. The shaded area is the region of integration for the determination of $G_{\pm}(\xi_0, \eta_0)$.

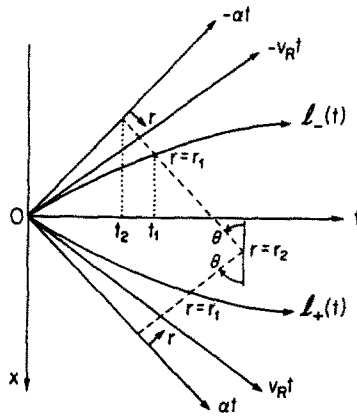


Fig. 5. Region of approximation of stresses used in (3.10) is shown by dashed lines. The angles $\theta = \tan^{-1}(v_R^{-1})$ or $\tan^{-1}(\alpha^{-1}) \cong \theta \cong \tan^{-1}(\beta^{-1})$.

From (3.7) we can write down expressions for F_+ and F_- outside the crack region, in terms of their values inside. These expressions are

$$F_+(\xi_0, \eta_0) = \frac{1}{\pi[\xi_0 - \xi_+(\eta_0)]^{1/2}} \int_0^{\xi_+(\eta_0)} \frac{F_+(\xi, \eta_0)[\xi_+(\eta_0) - \xi]^{1/2} d\xi}{(\xi_0 - \xi)}, \quad (3.8a)$$

$\xi_0 > \xi_+(\eta_0)$

and

$$F_-(\xi_0, \eta_0) = \frac{1}{\pi[\eta_0 - \eta_-(\xi_0)]^{1/2}} \int_0^{\eta_-(\xi_0)} \frac{F_-(\xi_0, \eta)[\eta_-(\xi_0) - \eta]^{1/2} d\eta}{(\eta_0 - \eta)}, \quad (3.8b)$$

$\eta_0 > \eta_-(\xi_0)$.

We let $\xi_0 \rightarrow \xi_+(\eta_0)^+$, and apply (3.1) and (3.3). Then

$$g_+ = \frac{1}{f_1(\dot{l}_+(t_0))} \left[\frac{\alpha - \dot{l}_+(t_0)}{2\alpha} \right]^{1/2} \int_0^{\xi_+(\eta_0)} \frac{F_+(\xi, \eta_0) d\xi}{[\xi_+(\eta_0) - \xi]^{1/2}}. \quad (3.9)$$

Equation (3.9) determines the condition for the extension of the positive edge of the crack in terms of the values of F_+ behind the crack. A similar equation for the condition that describes the negative edge of the crack can be obtained from (3.9) by replacing g_+ , $\dot{l}_+(t_0)$, F_+ , ξ_+ by g_- , $-\dot{l}_-(t_0)$, F_- and η_- respectively. From (2.5) and (2.6) it follows that a determination of F_{\pm} behind the crack edges requires that we know the values of $\sigma_2(x, t)$ in the same region. But σ_2 is known inside the torn region from the boundary condition (2.4). Outside the torn region σ_2 depends on the crack tip loci $l_{\pm}(t)$, which in turn depend on σ_2 , as in the case of anti-plane mode of fracture discussed in I and II. We interrupt this hierarchy of equations for the determination of σ_2 by assuming the following distribution of σ_2 outside the torn region. With reference to Fig. 5, we let

$$\sigma_2(x, t) = \frac{rg_+}{\pi r_1} [(r_1 - r)(\cos \theta + \dot{l}_+(t_1) \sin \theta)]^{-1/2} \quad (3.10a)$$

$$0 \leq r \leq r_1, \quad x > l_+(t)$$

$$F_-(x, t) = \frac{rg_{-,+}}{\pi r_1} [(r_1 - r)(\cos \theta + \dot{l}_+(t_1) \sin \theta)]^{-1/2} \quad (3.10b)$$

$$0 \leq r \leq r_1, \quad x > l_+(t)$$

$$\sigma_2(x, t) = \frac{rg_-}{\pi r_1} [(r_1 - r)(\cos \theta - \dot{l}_-(t_1) \sin \theta)]^{-1/2} \quad (3.10c)$$

$$0 \leq r \leq r_1, \quad x < l_-(t)$$

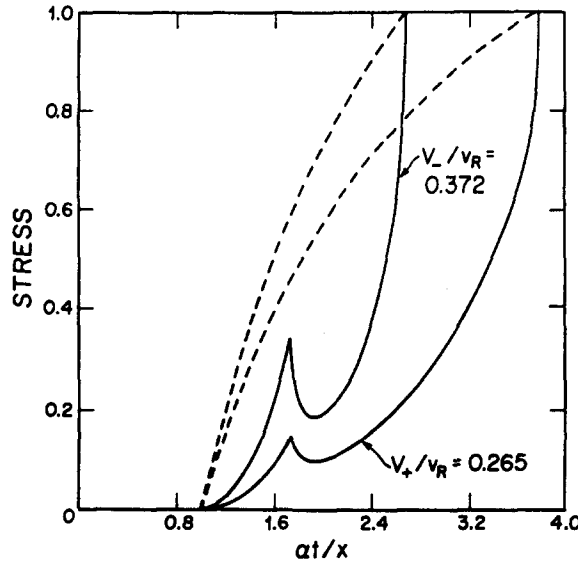


Fig. 6. Exact (solid) and approximate (dashed) stress distribution scaled with respect to the stresses at the edges of the crack for self-similar in-plane propagation. $V_+/v_R = 0.265$ and $V_-/v_R = 0.372$. The cusps in the exact solution are due to the discontinuous derivatives at the S-wave front.

$$F_+(x, t) = \frac{rg_{+,-}}{\pi r_1} [(r_1 - r)(\cos \theta - \dot{l}_-(t) \sin \theta)]^{-1/2} \quad (3.10d)$$

$$0 \leq r \leq r_1, \quad x < l_-(t).$$

Equations (3.10) have the appropriate singular behavior of the functions F_{\pm} , σ_2 as $r \rightarrow r_1$ and also satisfy the condition of zero stresses on the P-wave fronts. However, they do not reflect the discontinuous derivative at the S-wave fronts (Appendix and Fig. 6). In I and II we have investigated the validity of this approximation in the case of anti-plane strain crack propagation; this approximation yields a very good estimate of the cohesive forces except for very slow rates of extension of the crack. In the next section, we determine the equations of motion of the crack tips for general distribution of cohesion and dynamic friction. Then we discuss the special case of self-similar uniform bilateral in-plane crack. The latter problem has an exact analytical solution (see Appendix) which can be used to gauge the range of validity of the approximation (3.10).

4. EQUATIONS OF MOTION OF THE CRACK TIP. GENERAL CASE

In what follows, we scale all the velocities with respect to α . We first compute the tearing loci by ignoring the back edge radiation, which implies that for the determination of the location of the positive edge we assume that the negative edge extends with the P-wave velocity and vice versa. In making this assumption we may violate restrictions on the crack speed we may invoke later, such as one in which the crack velocity is less than the Rayleigh wave velocity. Nevertheless this restriction provides useful initial estimates for the function l_+ . From (2.6a), we have

$$F_+(x, t) = -p(x, t) + c \frac{\partial}{\partial t} \int_0^{\frac{x+t}{1+v_R^{-1}}} p(x - \eta, t - v_R^{-1}\eta) d\eta$$

$$+ \frac{1}{2\pi} \int_1^{\beta^{-1}} \lambda(s) \frac{\partial}{\partial t} \int_0^{\frac{x+t}{1+s}} p(x - \eta, t - s\eta) d\eta ds$$

$$= -f_+(x, t), \quad x < l_+(t) \quad (4.1)$$

where c is the constant $(v_R^{-1} - 1)^{1/2}(v_R^{-1} - \beta^{-1})^{1/2}/S(-v_R^{-1})$ and

$$\lambda(s) = \frac{\{1/S(-s)\}(s - 1)^{1/2}(\beta^{-1} - s)^{1/2}}{(v_R^{-1} - s)} \tag{4.2}$$

Hence as an initial approximation, the equation of motion of the positive edge of the crack (II) is

$$g_{+,+}^{(m)} \left[\frac{2}{(1 - l_+)} \right]^{1/2} = \int_0^{\xi_+(\eta_0)} \frac{f_+(\xi, \eta_0) d\xi}{(\xi_+ - \xi)^{1/2}}$$

which, using (3.3), becomes

$$\frac{2^{1/2}(1 - l_+/\beta)^{1/2}g_+}{S(-l_+^{-1})(1 - l_+/v_R)} = \int_0^{\xi_+(\eta_0)} \frac{f_+(\xi, \eta_0) d\eta}{(\xi_+ - \xi)^{1/2}} \tag{4.3}$$

Equations (4.1) and (4.3) plus an initial condition $l_+ = v_R$, completely determines the initial estimate of $l_+(t)$. We find in Section V below that self-similar cracks extend with velocities less than or equal to the Rayleigh wave velocity. We can not state that this is the case for later histories of inhomogeneous crack propagation, in which radiated P - and S -waves may trigger motions in advance of the Rayleigh wave front, but for the initial phases of the rupture, our initial condition suffices. Similarly, we can determine initial estimates of $l_-(t)$. The quantity $S(-v^{-1})$ is defined in (2.9) and is a smoothly varying function in the range $0 \leq v \leq v_R$. This leads to the following approximation

$$S(-v^{-1}) = \sum_{i=0}^5 a_i v^i, \quad 0 \leq v \leq v_R \tag{4.4}$$

where

$$\begin{aligned} a_0 &= 0.9977096 \\ a_1 &= 0.6056030 \\ a_2 &= -5.8835644 \\ a_3 &= 45.2408603 \\ a_4 &= 125.7868148 \\ a_5 &= 129.1117385 \end{aligned} \tag{4.5}$$

with a maximum error of 0.97%. For given x and t , l_+ can now be obtained from (4.3) by a Newton-Raphson method and hence we can solve (4.3) by a Runge-Kutta procedure.

If we wish to take into account the influence of the back edge radiation on the determination of the locus of the positive edge $l_+(t)$, we replace the negative edge by its initial estimate and then use (3.9) as the fracture criterion. The integral on the right hand side of (3.9) can be split into two parts, one inside the torn region and the other outside it. Outside the torn region we use (3.10d) and (3.3). Inside the torn region $F_+(x, t)$ may be obtained as follows. From (2.5)

$$\sigma_2^{(1)}(x, t, s) = \frac{\partial}{\partial t} \int_0^{\frac{x+t}{1+s}} \sigma_2(x - \eta, t - s\eta) d\eta, \quad x < l_+(t) \tag{4.6}$$

where the upper limit corresponds to the *P*-wave front. With reference to Fig. 5 and using (3.10d),

$$\int_0^{\frac{x+t}{1+s}} \sigma_2(x - \eta, t - s\eta) d\eta = \cos \theta \left[\int_{r_1}^{r_2} \sigma_2 dr + \frac{4r_1^{1/2}g_-}{3\pi(\cos \theta - \dot{l}_- \sin \theta)^{1/2}} \right]$$

where $\theta = \tan^{-1} s$. This gives

$$\begin{aligned} \sigma_2^{(1)}(x, t; s) = & -\cos \theta \left[\int_{r_1}^{r_2} \dot{p} dr + \dot{r}_2 p(r_2) - \dot{r}_1 p(r_1) \right. \\ & - \frac{2\dot{r}_1 g_-}{3r_1^{1/2}[\cos \theta - \dot{l}_-(t_1) \sin \theta]^{1/2}} - \frac{4r_1 \dot{g}_- - \dot{x}_1}{3[\cos \theta - \dot{l}_-(t_1) \sin \theta]^{1/2}} \\ & \left. + \frac{2r_1^{1/2}g_- \dot{l}_- \ddot{l}_-(t_1)}{3[\cos \theta - \dot{l}_-(t_1) \sin \theta]^{3/2}} \right] \end{aligned} \quad (4.7)$$

where x_1, t_1 are the values of x, t at $r = r_1$ (Fig. 5).

By substituting (4.7) in equation (2.6a) we can determine $F_+(x, t)$ inside the torn region $l_-(t) < x < l_+(t)$. Similarly we can determine $F_-(x, t)$ inside the torn region. Equations (3.9) and (3.3) now give the equations of motion for the determination of the unknown functions $l_{\pm}(t)$ when g_{\pm} and $p(x, t)$ are given functions. The procedure outlined in this paragraph can be repeated for the positive and negative edges alternately until the solutions for l_{\pm} converge. Usually three to four iterations are sufficient to achieve a reasonable degree of accuracy.

As we have noted, the success of this procedure to determine the crack tip loci depends strongly on the validity of (3.10). In the next section we compare the result obtained by using (3.10) with exact analytical solutions which can be derived for restricted problems having self-similar properties.

3. UNIFORM PROPAGATION OF IN-PLANE BILATERAL CRACK

It has been shown in Appendix I, that a spontaneous bilateral crack will grow with constant velocities at the edges if it has the following distribution of cohesions g_{\pm} and dynamic stress drop $p(x, t)$.

$$\begin{aligned} g_+ &= \alpha_+ x^{1/2}, & x > 0 \\ g_- &= \alpha_- (-x)^{1/2}, & x < 0 \\ p(x, t) &= p_0 \end{aligned} \quad (5.1)$$

where α_{\pm} and p_0 are constants. Let the crack tip loci be given by $|\dot{l}_{\pm}| = V_{\pm}$ where V_{\pm} are constants. We determine the relations between α_{\pm} and V_{\pm} for this case using (3.10) and compare with the exact analytical result (A14). Equation (A14) shows that $\alpha_+ < 0$ for $V_+ > v_R$ and $\alpha_+ \geq 0$ for $V_+ \leq v_R$. Hence if g_{\pm} is a measure of the material properties at the edges of the crack, then $g_{\pm} > 0$, which implies $V_{\pm} \leq v_R$. Thus the extension rates for self-similar cracks lie between zero and the Rayleigh wave velocity. In general, the greater the coefficients of cohesion α_{\pm} , the slower the rates of extension of the edges. This example is therefore a test which identifies the region of validity of (3.10). From (2.6), (3.10) and (5.1), F_{\pm} are constants inside the crack region $-V_-t < x < V_+t$.

$$\begin{aligned} -F_{\pm} = p_{\pm}^{(m)} = & p_0 \left[1 + f_5(V_{\mp}, v_R^{-1})f_2(v_R^{-1}) + \int_1^{\beta^{-1}} f_3(s)f_5(V_{\mp}, s) ds \right] \\ & + \alpha_{\pm} \left[f_4(V_{\mp}, v_R^{-1})f_2(v_R^{-1}) + \int_1^{\beta^{-1}} f_3(s)f_4(V_{\mp}, s) ds \right]. \end{aligned} \quad (5.2)$$

In this equation

$$\begin{aligned}
 f_2(x) &= \frac{[(x - 1)(x - \beta^{-1})]^{1/2}}{S(-x)} \\
 f_3(x) &= \frac{1}{2\pi} \left\{ \frac{1}{S(-s)} \right\} [(x - 1)(\beta^{-1} - x)]^{1/2} \\
 f_4(x, y) &= \frac{4[x(1 - x)]^{1/2}}{3\pi(1 + y)^{1/2}(1 + xy)^{3/2}} \\
 f_5(x, y) &= -\frac{x}{1 + xy}.
 \end{aligned}
 \tag{5.3}$$

From (3.9), (3.10), (5.1) and (5.2), it can be shown that (II)

$$\begin{aligned}
 \alpha_{+,+}^{(m)} \left(\frac{1 - b}{1 - V_+} \right)^{1/2} &= 2(1 - ab)^{1/2} p_+^{(m)} - \frac{\alpha_{+,-}^{(m)}}{\pi} \left(\frac{b(1 - a)}{1 + V_-} \right)^{1/2} f(A) \\
 \alpha_{-,-}^{(m)} \left(\frac{1 - a}{1 - V_-} \right)^{1/2} &= 2(1 - ab)^{1/2} p_-^{(m)} - \frac{\alpha_{-,+}^{(m)}}{\pi} \left[\frac{a(1 - b)}{1 + V_+} \right]^{1/2} f(A)
 \end{aligned}
 \tag{5.4}$$

where $g_{\pm,\pm}^{(m)} = \alpha_{\pm,\pm}^{(m)} |x|^{1/2}$ and

$$\begin{aligned}
 a &= \frac{1 - V_-}{1 + V_-} \\
 b &= \frac{1 - V_+}{1 + V_+} \\
 A &= \frac{1}{ab}, \quad f(A) = - \left[A^{1/2} + \frac{1 + A}{2} \cosh^{-1} \left(\frac{1 + A}{A - 1} \right) \right].
 \end{aligned}$$

Using (3.3) and (5.1), (5.4) can be written as

$$\begin{aligned}
 \bar{\alpha}_+ c_{11} + \bar{\alpha}_- c_{12} &= c_{13} \\
 \bar{\alpha}_+ c_{21} + \bar{\alpha}_- c_{22} &= c_{23}
 \end{aligned}
 \tag{5.5}$$

where $\bar{\alpha}_{\pm} = \alpha_{\pm}/p_0$ and

$$\begin{aligned}
 c_{11} &= \left(\frac{1 - b}{1 - V_+} \right)^{1/2} f_1(V_+) \\
 c_{12} &= \frac{1}{\pi} \left(\frac{b(1 - a)}{1 + V_-} \right)^{1/2} \left[f(A)f_1(-V_-) - 2(1 - ab)^{1/2} [f_4(V_-, v_{\bar{R}}^{-1})f_2(v_{\bar{R}}^{-1}) \right. \\
 &\quad \left. + \int_1^{\beta^{-1}} f_3(s)f_4(V_-, s) ds \right] \\
 c_{13} &= 2(1 - ab)^{1/2} \left[1 + f_5(V_-, v_{\bar{R}}^{-1})f_2(V_{\bar{R}}^{-1}) \right. \\
 &\quad \left. + \int_1^{\beta^{-1}} f_3(s)f_5(V_-, s) ds \right]
 \end{aligned}$$

and c_{21}, c_{22}, c_{23} can be obtained from c_{11}, c_{12}, c_{13} by replacing V_-, a, b by V_+, b, a respectively.

For given values of V_{\pm} , we obtain α_{\pm} from (5.5). The approximate solution (5.5) is given in Fig. 7 by the dashed curves. The solid curves in Fig. 7 represent the exact

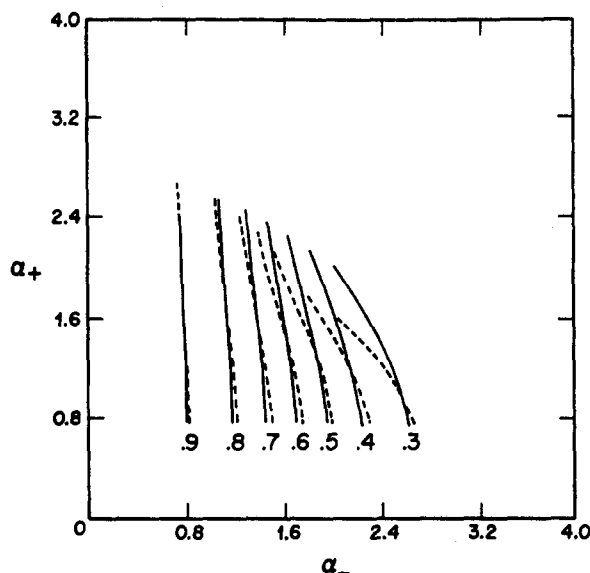


Fig. 7. Cohesive coefficients versus rupture speeds for the case of self-similar in-plane crack propagation. Solid lines are the exact solution (A14) while the dashed lines are the solution obtained by using the approximation (3.10). The numerical entries are the ratios V_-/v_R .

analytical solution obtained from (A14). There is a good agreement between the two solutions except at low rupture speeds. This indicates that (3.10) is a good approximation especially when we are interested in determining the tearing loci for rupture speeds that are not small. It should be emphasized here that the exact nature of the stress distribution is not displayed in (3.10). This is clear when we compare (3.10) with the exact stress distribution (A12) in the back edges. Thus to determine the exact stress distribution in the back edge region for slow extension of the crack, we represent the back edge stresses scaled with respect to the stresses at the respective edges by two separate functions, one in the region $1 \cong x/t \cong \beta$ and the other in the region $\beta \cong x/t \cong |\dot{l}_{\pm}|$. Once the crack tip loci have been obtained using (3.10) and the method outlined here, simultaneous iterations should be performed to correct the tearing loci and the back edge stresses. For high rupture speeds, the corrections to l_{\pm} are small while these corrections are significant for low rupture speeds. For the case of anti-plane crack propagation, these corrections have been given earlier in II and will be given separately for the in-plane cracks.

In general, the problem of spontaneous bilateral crack propagation is a complex non-linear problem. All attempts so far in the literature have focussed on purely numerical solutions to the problem. We have endeavored to show that an approximation to the stresses in the back edge region proves to be effective for the determination of the rupture loci. It works well for both anti-plane and in-plane shear crack propagation especially for high crack speeds. The exact stress distribution in the back edge region is more complex for the in-plane problem than for the anti-plane problem. In any case, both the exact back-edge stresses and the rupture loci can be obtained by the method discussed here. To incorporate the derivative discontinuity in the back-edge stresses, it is necessary to represent this by a function which has piecewise continuous derivatives in the two back edge regions that are separated by the S -wave front.

REFERENCES

1. R. Burridge and G. S. Halliday, Dynamic shear cracks with friction as models for shallow focus earthquakes. *Geophys. J. Roy. Astr. Soc.* **25**, 261 (1971).
2. S. Das and K. Aki, A numerical study of two-dimensional spontaneous rupture propagation. *Geophys. J. Roy. Astr. Soc.* **50**, 643 (1977).
3. D. J. Andrews, Rupture velocity of plane-strain shear cracks. *J. Geophys. Res.* **81**, 5679 (1976).
4. L. Knopoff and A. K. Chatterjee, Unilateral extension of a two-dimensional shear crack under the influence of cohesive forces. *Geophys. J. Roy. Astr. Soc.* **68**, 7 (1982).

5. A. K. Chatterjee and L. Knopoff, Bilateral propagation of a spontaneous two-dimensional anti-plane shear crack under the influence of cohesion. *Geophys. J. Roy. Astr. Soc.* **73**, 449 (1983).
6. B. V. Kostrov, On the crack propagation with variable velocity. *Int. J. Fracture* **11**, 47 (1975).
7. R. Burridge, G. Conn and L. B. Freund, The stability of a rapid mode II shear crack with finite cohesive traction. *J. Geophys. Res.* **84**, 2210 (1979).
8. Y. Y. Kagan and L. Knopoff, Spatial distribution of earthquakes: the two-point correlation function. *Geophys. J. Roy. Astr. Soc.* **62**, 303 (1980).
9. R. S. Sayles and T. R. Thomas, Surface topography as a nonstationary random process. *Nature* **271**, 431 (1978).
10. B. T. Brady, Theory of earthquakes. *Pure and Appl. Geophys.* **112**, 701 (1974).
11. R. Burridge, Admissible speeds for plane-strain self-similar shear cracks with friction but lacking cohesion. *Geophys. J. Roy. Astr. Soc.* **35**, 439 (1973).
12. A. T. de Hoop, Representation theorems for the displacement of an elastic solid and their application to elastodynamic diffraction theory. *Sci. D. Thesis*, Technische Hogeschool, Delft (1958).
13. V. Smirnoff and S. Sobolev, Sur une methode nouvelle dans le probleme plan des vibrations elastiques. *Trudy Seysmologicheskoy instituta*, No. 20 (1932).
14. G. P. Cherepanov and E. F. Afanas'ev, Some dynamic problems of the theory of elasticity—a review. *Int. J. Engng Sci.* **12**, 665 (1974).
15. B. V. Kostrov, Self-similar problems of propagation of shear cracks. *PMM* **28**, 889 (1964).

APPENDIX

Exact solution of uniformly propagating bilateral crack

Let an in-plane bilateral crack initiate along the line $x = z = 0$ and propagate uniformly with speeds V_{\pm} along the $\pm x$ -axis. At any time t , the displacement components are $u = u(x, z, t)$, $v = 0$ and $w = w(x, z, t)$ along the x, y, z axis respectively. In terms of the displacement potentials Φ and Ψ , u and w may be written as

$$\begin{aligned} u(x, z, t) &= \Phi_{,x} + \Psi_{,z} \\ w(x, z, t) &= \Phi_{,z} - \Psi_{,x} \end{aligned} \tag{A1}$$

where Φ and Ψ satisfy the wave equations

$$\begin{aligned} \alpha^{-2}\ddot{\Phi} &= \Phi_{,xx} + \Phi_{,zz} \\ \beta^{-2}\ddot{\Psi} &= \Psi_{,xx} + \Psi_{,zz} \end{aligned} \tag{A2}$$

Let the superscripts (1) and (2) indicate the contribution to the field quantities by Φ and Ψ respectively. Then $\dot{u}^{(1)}$, $\dot{w}^{(1)}$, $\sigma_{xz}^{(1)}$ and $\sigma_{zz}^{(1)}$ all satisfy the wave equation with speed α while those with superscript (2) satisfy the wave equation with speed β . We solve the problem with the boundary conditions

$$\begin{aligned} \sigma_{zz} &= 0, \quad z = 0 \\ \sigma_{xz} &= -p_0 \text{ (constant)}, \quad -V_-t \leq x \leq V_+t, \quad z = 0 \\ u &= 0, \quad |x| \geq V_{\pm}t, \quad z = 0 \end{aligned} \tag{A3}$$

Since the problem is self-similar $\dot{u}^{(1)}$, etc. are all homogeneous functions of degree zero. By the functionally invariant method of Smirnoff and Sobolev [13] (see also [14]), each of these quantities can be represented by a function $f(\tau)$ where $t = x\tau + z(c^{-2} - \tau^2)^{1/2}$ where $c = \alpha$ or β according as the superscript is (1) or (2). Thus we have

$$\begin{aligned} \dot{u}^{(1),(2)} &= \text{Im}[U^{(1),(2)}(\tau^{(1),(2)})] \\ \dot{w}^{(1),(2)} &= \text{Im}[W^{(1),(2)}(\tau^{(1),(2)})] \\ \sigma_z^{(1),(2)} &= \sigma_{zz}^{(1),(2)} = \text{Im}[\Sigma_z^{(1),(2)}(\tau^{(1),(2)})] \\ \sigma_{xz}^{(1),(2)} &= \text{Im}[T_{xz}^{(1),(2)}(\tau^{(1),(2)})] \end{aligned} \tag{A4}$$

where $\tau^{(1)}$ and $\tau^{(2)}$ are functions of x, z, t which satisfy

$$\begin{aligned} t &= x\tau^{(1)} + z(\alpha^{-2} - \tau^{(1)2})^{1/2} \\ t &= x\tau^{(2)} + z(\beta^{-2} - \tau^{(2)2})^{1/2} \end{aligned} \tag{A5}$$

On the crack plane $z = 0$, $\tau^{(2)} = \tau^{(1)} = t/x$. From the equations of motion and stress-displacement relations, we have

$$\begin{aligned} \dot{w} &= \sigma_{xz,x} + \sigma_{z,z} \\ \dot{\sigma}_z &= \mu \left[\left(\frac{\alpha^2}{\beta^2} - 2 \right) \dot{u}_{,x} + \frac{\alpha^2}{\beta^2} \dot{w}_{,z} \right] \\ \dot{\sigma}_{xz} &= \mu(\dot{u}_{,z} + \dot{w}_{,x}). \end{aligned} \tag{A6}$$

From (A3)–(A6), it can be shown that all the eight unknown functions $U^{(1),(2)}$, etc. are related to only

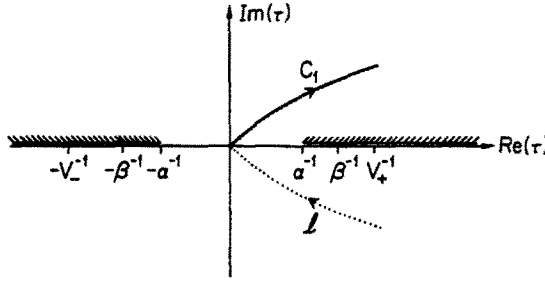


Fig. 8. Paths of integration in the complex τ -plane used in (A9). Branch cuts extend to infinity from $\pm\alpha^{-1}$ and l is the path along the dotted lines.

one unknown function $V(\tau)$ through the relations

$$\begin{aligned}
 U^{(1)'}(\tau) &= 2\beta^2\tau^2V'(\tau) \\
 U^{(2)'}(\tau) &= (1 - 2\beta^2\tau^2)V'(\tau) \\
 W^{(1)'}(\tau) &= 2\beta^2\tau(\alpha^{-2} - \tau^2)^{1/2}V'(\tau) \\
 W^{(2)'}(\tau) &= -\tau(1 - 2\beta^2\tau^2)(\beta^{-2} - \tau^2)^{-1/2}V'(\tau) \\
 T_{xz}^{(1)'}(\tau) &= -4\mu\beta^2\tau^2(\alpha^{-2} - \tau^2)^{1/2}V'(\tau) \\
 T_{xz}^{(2)'}(\tau) &= -\frac{4\mu\beta^2(\tau^2 - \beta^{-2}/2)^2V'(\tau)}{(\beta^{-2} - \tau^2)^{1/2}} \\
 \Sigma_z^{(1)'}(\tau) &= -\Sigma_z^{(2)'}(\tau) = -2\mu\tau(1 - 2\beta^2\tau^2)V'(\tau).
 \end{aligned} \tag{A7}$$

Following Kostrov [15], we take

$$V'(\tau) = A(V_+^{-1} - \tau)^{-1/2}(V_-^{-1} + \tau)^{-1/2} \tag{A8}$$

where A is an unknown constant to be determined from (A3). Substituting (A8) in (A7), we get the derivatives of all the functions $U^{(1)'}(\tau)$, etc. To integrate these functions, we note that in the complex τ -plane all these functions are regular with branch cuts along the real axis from $-\alpha^{-1}$ to $-\infty$ and α^{-1} to ∞ . Also the crack plane $z = 0$ corresponds to the real axis in the τ -plane with the origin representing $t = 0$. Since at $t = 0$, all the field quantities are zero, if $f(\tau)$ denotes any of the functions $U^{(1)}$, etc. we have

$$f(\tau) = \text{Im} \left[\int_{C_1} f'(\tau) d\tau \right] = \frac{1}{2i} \int_l f'(\tau) d\tau \tag{A9}$$

where the paths of integration C_1 and l are shown in Fig. 8.

The unknown constants A can now be determined from the boundary condition that on $z = 0$, $\sigma_{xz} = -p$, $-V_-t < x < V_+t$. This gives

$$-p_0 = 2i\mu\beta^2 \int_l \frac{R(\tau^2)V'(\tau) d\tau}{(\beta^{-2} - \tau^2)^{1/2}}.$$

Deforming the contour l as shown in Fig. 9 and replacing it by the dashed contour, we have

$$\begin{aligned}
 p_0 &= 2^{1/2}2\mu\beta^2A \int_0^\infty \frac{[(\tau^2 + \beta^{-2}/2)^2 - \tau^2(\alpha^{-2} + \tau^2)^{1/2}(\beta^{-2} + \tau^2)^{1/2}]}{(\beta^{-2} + \tau^2)^{1/2}[(V_-^{-2} + \tau^2)(V_+^{-2} + \tau^2)]^{3/4}} \\
 &\quad \times [(V_+^{-1}V_-^{-1} + \tau^2)(1 + B)^{1/2} - \tau |V_+^{-1} - V_-^{-1}| (1 - B)^{1/2}] d\tau
 \end{aligned} \tag{A10}$$

where

$$B = \left[1 + \frac{\tau^2(V_+ - V_-)^2}{(1 + \tau^2V_+V_-)} \right]^{-1/2}.$$

(A10) determines A and thus we have the complete exact solution to the problem.

Stresses outside the crack

From (A4) and (A7), the shear stress on the crack plane $z = 0$ is given by

$$\sigma_{xz}(x, 0, t) = -\text{Im} \left[\int_0^{x^+ + 0} \left\{ \tau^2(\alpha^{-2} - \tau^2)^{1/2} + \frac{(\tau^2 - \beta^{-2}/2)^2}{(\beta^{-2} - \tau^2)^{1/2}} \right\} \times \frac{d\tau}{[(V_+^{-1} - \tau)(V_-^{-1} + \tau)]^{3/2}} \right] \tag{A11}$$

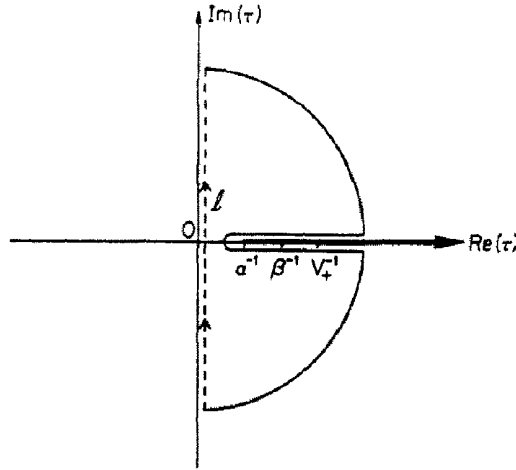


Fig. 9. The contour l (dashed line) in the complex τ -plane that can be used to derive (A10). The integrals over the arcs at infinity approach zero. The heavy solid line indicates the branch cut.

(A11) yields

$$\begin{aligned} \frac{\sigma_{xz}(x, 0, t)}{4\mu\beta^2 A} &= 0, \quad x > \alpha t \\ &= f_1\left(\frac{t}{x}\right), \quad \beta t \leq x \leq \alpha t \\ &= f_2\left(\frac{t}{x}\right), \quad \gamma t \leq x \leq \beta t \\ &= f_2(\gamma^{-1}) + g_1\left(\frac{t}{x}\right) - g_1(\gamma^{-1}) - \int_{\gamma^{-1}} \frac{g_2(\tau) d\tau}{(V_+^{-1} - \tau)^{1/2}}, \quad x < \gamma t \end{aligned} \tag{A12}$$

where $\gamma^{-1} = (\beta^{-1} + V_+^{-1})/2$ and the functions f_1, f_2, g_1, g_2 are given by

$$\begin{aligned} f_1\left(\frac{t}{x}\right) &= \int_{\alpha^{-1}}^{\frac{t}{x}} \frac{\tau^2(\tau^2 - \alpha^{-2})^{1/2} d\tau}{(V_-^{-1} + \tau)^{3/2}(V_+^{-1} - \tau)^{3/2}} \\ f_2\left(\frac{t}{x}\right) &= f_1\left(\frac{t}{x}\right) - \int_{\beta^{-1}}^{\frac{t}{x}} \frac{(\tau^2 - \beta^{-2}/2)^2 d\tau}{(\tau^2 - \beta^{-2})^{1/2}(V_-^{-1} + \tau)^{3/2}(V_+^{-1} - \tau)^{3/2}} \\ g_1(\tau) &= 2 \left[\tau^2(\tau^2 - \alpha^{-2})^{1/2} - \frac{(\tau^2 - \beta^{-2}/2)^2}{(\tau^2 - \beta^{-2})^{1/2}} \right] (V_-^{-1} + \tau)^{-3/2} (V_+^{-1} - \tau)^{-1/2} \\ g_2(\tau) &= (V_-^{-1} + \tau)^{-3/2} \left[\frac{\tau(6V_-^{-1}\tau^2 + 3\tau^3 - \alpha^{-2}\tau - 4\alpha^{-2}V_-^{-1})}{(\tau^2 - \alpha^{-2})^{1/2}} \right. \\ &\quad \left. + \frac{(\tau^2 - \beta^{-2}/2)}{(\tau^2 - \beta^{-2})^{3/2}} \left(\frac{5}{2} \beta^{-2}\tau^2 + 7\beta^{-2}V_-^{-1}\tau + \frac{3}{2} \beta^{-4} - 3\tau^4 - 6V_-^{-1}\tau^3 \right) \right]. \end{aligned}$$

Letting $x \rightarrow V_+ T^+$, we have, from (A12)

$$\sigma_{xz} = \frac{\alpha_+ x^{1/2}}{\pi(x - V_+ t)^{1/2}} + O(1) \tag{A13}$$

where

$$\alpha_+ = \frac{8\pi\mu\beta^2 A V_+^{-1}}{(1 + V_+/V_-)^{3/2}(1 - V_+^2/\beta^2)^{1/2}} \left[\{(1 - V_-^2/\alpha^2)(1 - V_+^2/\beta^2)\}^{1/2} - \{1 - V_+^2/(2\beta^2)\}^2 \right] \tag{A14}$$

α_- can be obtained from (A14) by an interchange of V_+ and V_- .